Free-carrier effect on exciton dynamics in GaAs/$Al_xGa_{1-x}As$ quantum wells

B. M. Ashkinadze, E. Linder, E. Cohen, and Arza Ron
Solid State Institute, Technion–Israel Institute of Technology, Haifa 32000, Israel

L. N. Pfeiffer
AT&T Bell Laboratories, Murray Hill, New Jersey 07974
(Received 20 September 1994)

We report on a strong modulation of the resonantly excited ($e1$:hh1)1S exciton photoluminescence and LO-phonon Raman scattering by an additional, weak, above-gap radiation at low temperatures. These effects are attributed to the interaction between excitons and cold, free carriers (in the e-h pair density range of $10^5 < n < 10^7$ cm^{-2}) that causes an exciton population redistribution and an increased dephasing rate. The analysis indicates that localized and delocalized exciton states span the same spectral range. It also yields the spectral dependence of the additional exciton dephasing that is due to the interaction with free carriers.

The low-temperature optical and electrical properties of semiconductor quantum wells (QW's) are determined, to a large extent, by the in-plane translational motion of e-h pairs in the spatially fluctuating potential. In particular, luminescence and light scattering that are resonantly excited near the ($e1$-hh1) band gap are strongly affected by the dynamics of the photoexcited e-h pairs, both excitons and free carriers. These include scattering or localization by interface potential fluctuations and acoustic-phonon scattering processes.[1,2] Experimentally, these processes are investigated by extracting the temporal and spectral dependence of the exciton population [within the inhomogeneously broadened ($e1$:hh1)1S band] and of the exciton dephasing rate.[3–6] The latter was measured (as the homogeneous width Γ_h) for various GaAs/$Al_xGa_{1-x}As$ QW's by several techniques and was found to vary from $\Gamma_h(E) \sim 0.03$ meV in the low-energy tail of the ($e1$:hh1)1S band to ~ 2 meV in the high-energy part (at low temperatures). This was explained by an increased exciton transfer rate with increasing exciton energy E.

Upon increasing the photoexcitation intensity, several new effects were observed and attributed to exciton-exciton and exciton–free-carrier interactions. The photoluminescence (PL) rise time was found[7–9] to decrease with increased e-h pair density in the range $n \sim (2\times10^8)$–10^{10} cm^{-2} and was explained by an increased exciton cooling rate. The PL decay was found[10] to be nonexponential for $n \sim (1.5$–$8)\times10^8$ cm^{-2} and this was explained by a time-dependent Γ_h (due to exciton-exciton scattering). A linear dependence of Γ_h on n was observed, by using the time-resolved four-wave-mixing techniques,[4,11] in the range $n \sim 10^9$–(2×10^{10}) cm^{-2}. It was also found that the exciton–free-carrier scattering is an order of magnitude more effective in exciton dephasing than exciton-exciton scattering. No spectral dependence of the high-density excitons or free carriers on the exciton decay rate and Γ_h was reported.

In this work we report on phenomena that result from the interaction of excitons with cold, free carriers in undoped GaAs/$Al_xGa_{1-x}As$ QW's that are photoexcited in the range of very low e-h pair densities ($10^5 < n < 10^7$ cm^2). The resonantly excited luminescence spectrum and the LO-phonon resonant Raman scattering (RRS) intensity are found to be affected by a weak, additional photoexcitation with (laser) energy above the ($e1$-hh1) band gap. These are observed in the limit of single-exciton–carrier scattering and are used to study the spectral dependence of the exciton–free-carrier interaction and its effects on the exciton population distribution and dephasing. The analysis indicates that excitons localized by interface potential fluctuations are affected by the interaction with free carriers and that their density of states spans the entire ($e1$:hh1)1S band. The photomodulation method introduced here also provides a direct determination of the ($e1$-hh1) band gap.

Several undoped GaAs/$Al_{0.33}Ga_{0.67}As$ multiple QW's were studied. They were all grown by molecular-beam epitaxy on (001)-oriented GaAs substrates and have well widths of 50, 70, and 100 Å and a barrier width of 200 Å. (Detailed microwave modulation, absorption, and polarization studies of the same QW's were reported previously.[12,13]) The samples were placed in an immersion-type Dewar and the temperature was varied in the range 1.8–30 K. They were simultaneously irradiated by two laser beams, both impinging on the same spot on the sample surface, in a backscattering geometry. One beam (of either a Ti:Al_2O_3 or a dye laser), denoted L_1, was tuned resonantly within the inhomogeneously broadened ($e1$:hh1)1S exciton band. It serves as the excitation source of both the exciton PL and the exciton-mediated LO-phonon RRS. Its intensity at the sample surface was varied in the range $I_{L_1} \sim 0.05$–5 W/cm^2 (generating a steady-state exciton density $n_{ex} \sim 10^5$–10^7 cm^{-2}). A second laser beam (either of a pyridine 2 dye laser or a He-Ne laser), denoted L_2, serves as a modulation source. Its energy was varied over a wide range $E_{L_1} < E_{L_2} < E_{L_1} + 0.3$ eV, where E_{L_1} is the L_1 laser energy. Its intensity was in the range $I_{L_2} \sim 0.01$–1 W/cm^2 and it was chopped at a frequency of 900 Hz. The light emitted from the photoexcited multiple QW's was moni-

tored by a double monochromator and the signal was processed by a lock-in amplifier. In the following we describe results obtained for the 50 Å multiple QW. Similar results were obtained for the other QW's.

The effect of an additional above-gap excitation on the PL spectral shape is shown and explained in Figs. 1(a) and 1(b). The PL spectrum, excited by L_1, is shown in Fig. 1(a) (solid line). When a cw L_2 is turned on, the PL spectral shape is modified (dotted line): the intensity decreases in the high-energy part and increases in the low-energy tail. In Fig. 1(b) the photomodulated PL (MPL) spectrum is shown by the solid line. It is obtained by first exciting simultaneously with a cw L_1 and a chopped L_2 and monitoring the PL at the modulation frequency (dashed line). From this spectrum we then subtract the PL spectrum excited only by the chopped L_2 (dotted line). The resulting spectrum is the net photomodulation effect, namely, the variation induced in the resonantly excited (with L_1) PL by the above-gap excitation (with L_2). It is observed that for given E_{L_1} and I_{L_1} the MPL spectral shape is independent of I_{L_2}. The integrated intensity of either the positive or the negative part of the MPL depends sublinearly on I_{L_2} ($I_{\mathrm{MPL}} \sim I_{L_2}^{1/2}$) and linearly on I_{L_1}. The maximal modulation depth is $\sim 25\%$ for $I_{L_2} \sim 1$ W/cm^2. Note that the PL intensity depends linearly on either I_{L_1} or I_{L_2} when they excite the QW separately.

In order to compare the MPL spectrum with that obtained in other modulation experiments, we show in Fig. 1(c) an example of a microwave modulated PL spectrum of the same sample.[12] The temperature-modulated spectrum[12] has a similar shape to that of Fig. 1(c), but is much weaker. It is clear that these modulations have an effect on the PL spectrum opposite that of photomodulation. The integrated MPL intensity decreases with increasing temperature until it vanishes at $T > 20$ K. Its temperature dependence has a single activation energy of 2.2 meV.

The dependence of the modulation effect on the energy of the additional photoexcitation E_{L_2} is studied in Fig. 2. A series of PL excitation (PLE) spectra is shown, all monitored at the peak of the PL band [at E_m, Fig. 2(a)]. The PLE spectrum, excited with a chopped L_2 and no L_1, is shown in Fig. 2(b). Then a cw L_1 is added at either $E_{L_1} = 1.635$ or 1.640 eV, resulting in the PLE spectra of Figs. 2(c) and 2(d), respectively. We note that all three PLE spectra are identical in the spectral range $E_{L_2} < 1.642$ eV, while large differences between them are found for higher E_{L_2}. This is better presented in Fig. 2(e), which shows the difference between the spectra shown in Figs. 2(b) and 2(c). The sharp decrease in the

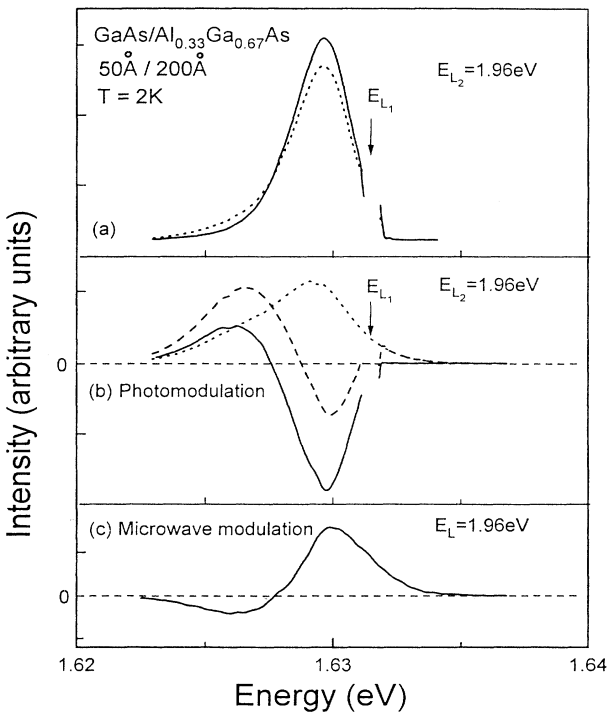

FIG. 1. (a) The (e1:hh1)1S PL band obtained under resonant excitation at $E_{L_1} = 1.631$ eV (solid line) and under an additional excitation at E_{L_2} (dotted line). (b) The photomodulated PL spectrum (solid line) is obtained by subtracting the PL spectrum excited at E_{L_2} (dotted line) from that excited at both E_{L_1} and E_{L_2} (dashed line). In all spectra, the cw L_1 laser intensity is 1.5 W/cm^2 and the chopped L_2 laser intensity is 0.2 W/cm^2. (c) The microwave-modulated PL spectrum.

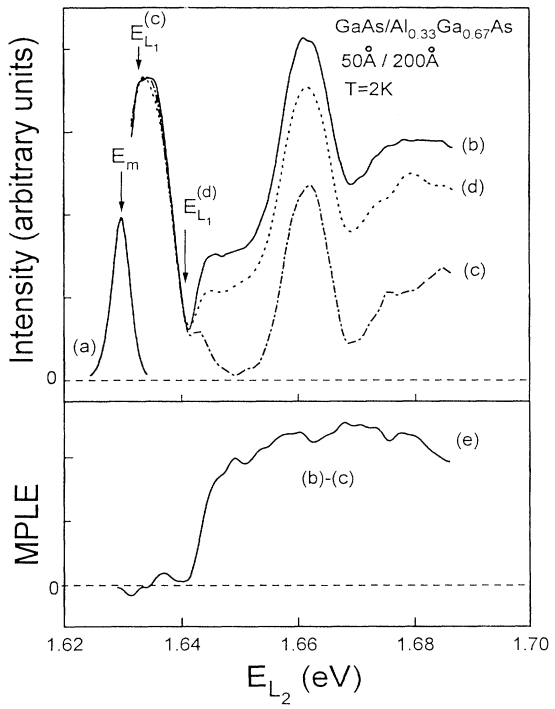

FIG. 2. PLE spectra monitored at the peak of the PL band [E_m in (a)]: Spectrum (b) is obtained without resonant excitation in the (e1:hh1)1S band, while spectra (c) and (d) are obtained with such excitations. (e) The photomodulated PLE spectrum. The laser intensities are the same as in Fig. 1.

PL intensity that sets in at $E_{L_2}=1.642$ eV will be shown below to provide a direct determination of the (e1-hh1) band gap.

Finally, we studied the photomodulated resonant Raman scattering (MRRS) profile. This was done by first measuring the intensity of the GaAs-like LO-phonon Raman line, excited by a cw L_1, and then its modulation by a chopped L_2, with $E_{L_2}=1.96$ eV. The MRRS is negative. Its intensity, divided by the corresponding RRS intensity, was measured for various E_{L_1} and is shown in Fig. 3(a). Also shown are the RRS profile [Fig. 3(b)] and the PLE spectrum [Fig. 3(c)] that is monitored at the PL peak (E_m). Note that a similar MRRS was obtained for $E_{L_2}=1.65$ eV, just above the band gap.

We interpret the effect of above-gap photomodulation on the PL spectral shape and RRS intensity as due to the interaction of localized excitons with cold, free carriers. The resonant L_1 excitation creates excitons only and these are distributed among the states that result from the perturbation on the exciton in-plane motion by the spatially fluctuating potential. This gives rise to the inhomogeneously broadened PL band. When L_2 is applied, additional excitons as well as free carriers are generated. The net effect of the L_2 photomodulation, as shown in Fig. 1(b), is an intensity decrease in the upper part of the PL band and an increase in its lower part. This pattern is observed when L_1 is tuned over the entire (e1:hh1)1S

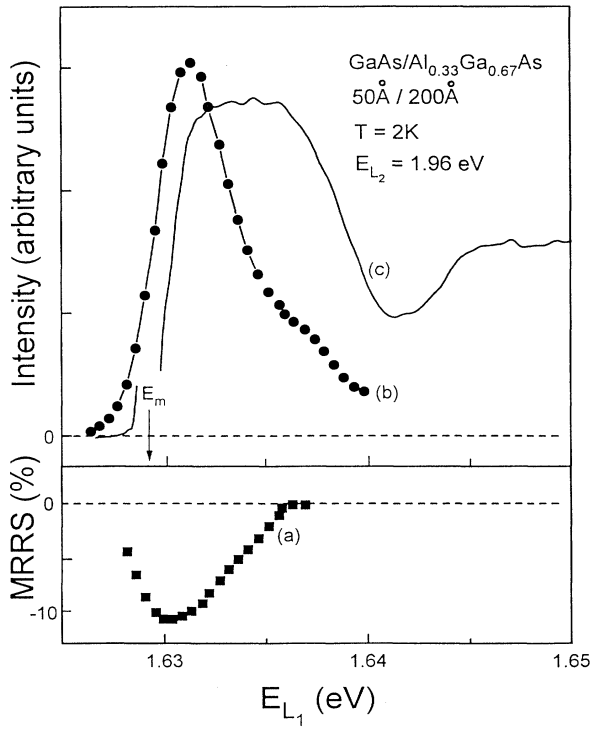

FIG. 3. (a) The photomodulated LO-phonon RRS profile. (b) The RRS profile (incoming beam resonance). (c) The PLE spectrum monitored at the peak of the PL band (obtained without excitation at E_{L_2}). The laser intensities are $I_{L_1}=2$ W/cm^2 and $I_{L_2}=0.5$ W/cm^2.

band. Carrier or lattice heating (by L_2) is ruled out since both microwave and temperature modulations produce the opposite effect[12] [Fig. 1(c)]. The modulated PLE spectra (Fig. 2) and the dependence $I_{\mathrm{MPL}} \propto I_{L_2}^{1/2}$ indicate that the MPL is caused by cold, free carriers that are generated by L_2. The sharp onset of modulation at $E_{L_2}=1.642$ eV coincides with the (e1-hh1) band gap deduced from the 1S-2S energy interval of the (e1:hh1) exciton.[13] The MPL intensity dependence of I_{L_2} is explained by the steady-state free-carrier density, when the formation of excitons is the limiting factor: $dn/dt=G_{L_2}-bn^2$ leads to $n=(G_{L_2}/b)^{1/2}$. Here G_{L_2} is the generation rate of e-h pairs and b is the exciton formation coefficient. In contrast to this dependence, we found that $I_{\mathrm{MPL}} \propto I_{L_1}$, namely, it is linearly dependent on the density of the resonantly generated excitons. We can therefore sum up the observed photomodulated PL intensity dependences as

$$I_{\mathrm{MPL}}=A(E_{L_1},E_{L_2})I_{L_1}I_{L_2}^{1/2} . \tag{1}$$

The physical mechanism that determines the MPL is represented by the $A(E_{L_1},E_{L_2})$ function and is based on the details of the exciton–free-carrier interaction. The following mechanisms are possible: (i) Free carriers induce an exciton transfer from one localized state into another. The carrier takes up the energy difference between the two exciton states in the inelastic scattering process. (ii) The carrier imparts some kinetic energy to the localized exciton, thus activating it into a delocalized state from which it is trapped into a lower-energy state. In either case, the excitons involved in the MPL effect must be localized; otherwise they would rapidly transfer by the dominant acoustic-phonon-assisted process and the population distribution will be that obtained under either L_1 or L_2 excitation. Considering the MPL spectral shape, it changes sign at the same energy as the microwave MPL spectrum [Figs. 1(b) and 1(c)]. This energy thus corresponds to localized excitons having exactly equal in (and out) transfer rates. Also, the decrease of the (integrated) MPL intensity with increasing temperature has an activation energy of 2.2 meV. This indicates that the localized excitons involved are a subset of the entire exciton population that cannot tunnel (within their radiative lifetime) unless they surmount a barrier of 2.2 meV. This must be taken as an average value, since the temperature dependence of the integrated MPL intensity is used.

The photomodulated RRS intensity renders further support to this analysis. The intensity of the LO-phonon scattering, which is resonantly excited at E_{L_1} (incoming beam resonance), is given by[2,14,15]

$$I_{\mathrm{RRS}}(E_{L_1})=B\int\int\frac{\Gamma_h(E)\rho(E)dEd\Gamma_h}{(E-E_{L_1})^2+\Gamma_h^2(E)} , \tag{2}$$

where $\rho(E)$ is the exciton density of states and B contains the exciton-photon and exciton-photon interaction factors. The damping factor is taken[15,16] as the dephasing rate of the exciton in the state with energy E. There is a

distribution of $\Gamma_h(E)$, for excitons with the same E, due to the different dynamic processes that they undergo. This leads to the integration over all $\Gamma_h(E)$. Clearly the highest contribution to I_{RRS} comes from states with the smallest $\Gamma_h(E)$. Then the integration in Eq. (2) can be approximated[2,6] as

$$I_{\mathrm{RRS}}(E_{L_1}) \sim B \frac{\pi\rho(E_{L_1})}{\Gamma_h(E_{L_1})} . \tag{3}$$

Under L_1 excitation, only exciton–acoustic-phonon scattering contributes to the damping (at a rate of Γ_h^{ac}). With L_2 photomodulation, exciton–free-carrier scattering is added:

$$\Gamma_h(E) = \Gamma_h^{\mathrm{ac}}(E) + \Gamma_h^{\mathrm{fc}}(E) . \tag{4}$$

Then, using Eq. (3),

$$\frac{I_{\mathrm{MRRS}}(E_{L_1})}{I_{\mathrm{RRS}}(E_{L_1})} = -\frac{\Gamma_h^{\mathrm{fc}}(E_{L_1})}{\Gamma_h(E_{L_1})} . \tag{5}$$

Consequently, the MRRS profile of Fig. 3(a) yields the (relative) change in the dephasing rate due to the exciton–free-carrier interaction. This profile extends to energies higher than the PL band. Previous studies[13,17] of the spectral and temporal dependences of the exciton circular and linear PLE polarizations indicated that they are due to delocalized excitons. These are excitons that can move over large interface islands with an approximately defined in plane $\mathbf{k}_{\parallel}$. Therefore, they are efficiently scattered by acoustic phonons and thus have a large Γ_h^{ac}. We conclude that the largest contribution to the MRRS must be due to localized excitons since they have a slow acoustic-phonon-assisted transfer rate into lower-energy states and are most sensitive to free-carrier scattering. The MRRS profile thus shows that both localized and delocalized excitons share the same spectral range of the entire inhomogeneously broadened ($e1$:hh1)1S band. A similar conclusion has been reached by Shields *et al.*,[6] who analyzed the spectral dependence of the exciton dephasing time.

In summary, we showed, by using a relatively simple photomodulation technique, that free carriers interact with excitons in GaAs/$Al_xGa_{1-x}As$ QW's even for extremely low e-h pair densities. This leads to effects that are observed in the limit of single-scattering events between the elementary excitations of QW's: a redistribution of the exciton population among the states that results from the interface roughness and an additional exciton dephasing that reduces the LO-phonon RRS intensity. We argue that the most affected excitons are those in localized states and that their density spans the entire ($e1$:hh1)1S band. This leads to the important conclusion that in QW's, localized and delocalized exciton states coexist in the same spectral range.

The research at Technion was done in the Barbara and Norman Seiden Center for Advanced Optoelectronics and was supported by the Basic Research Foundation administered by the Israel Academy of Sciences and Humanities and by the Foundation Rich, France.

[1]J. Hegarty and M. D. Sturge, J. Opt. Soc. Am. B **2**, 1153 (1985).
[2]T. Takagahara, Phys. Rev. B **31**, 6552 (1985); J. Lumin. **44**, 347 (1989).
[3]J. Hegarty and M. D. Sturge, Surf. Sci. **196**, 555 (1988).
[4]J. Kuhl, A. Honold, L. Schultheis, and C. W. Tu, Festkörperprobleme **29**, 157 (1989).
[5]H. Stolz, Festkörperprobleme **31**, 219 (1991).
[6]A. J. Shields, G. O. Smith, E. J. Mayer, R. Eccleston, J. Kuhl, M. Cardona, and K. Ploog, Phys. Rev. B **48**, 17 338 (1993).
[7]T. C. Damen, J. Shah, D. Y. Oberli, D. S. Chemla, J. E. Cunningham, and J. M. Kuo, Phys. Rev. B **42**, 7434 (1990).
[8]R. Eccleston, R. Strobel, W. W. Rühle, J. Kuhl, B. F. Feuerbacher, and K. Ploog, Phys. Rev. B **44**, 1395 (1991).
[9]Ph. Roussignol, C. Delalande, A. Vinattieri, L. Carraresi, and M. Colocci, Phys. Rev. B **45**, 6965 (1992).
[10]R. Eccleston, B. F. Feuerbacher, J. Kuhl, W. W. Rühle, and K. Ploog, Phys. Rev. B **45**, 11 403 (1992).
[11]A. Honold, L. Schultheis, J. Kuhl, and C. W. Tu, Phys. Rev. B **40**, 6442 (1989).
[12]B. M. Ashkinadze, E. Cohen, Arza Ron, and L. N. Pfeiffer, Phys. Rev. B **46**, 10 613 (1993).
[13]A. Frommer, E. Cohen, Arza Ron, and L. N. Pfeiffer, Phys. Rev. B **48**, 2803 (1993); A Frommer, Arza Ron, E. Cohen, J. A. Kash, and L. N. Pfeiffer, *ibid.* **50**, 11 833 (1994).
[14]D. Gershoni, E. Cohen, and Arza Ron, Phys. Rev. Lett. **56**, 2211 (1986).
[15]A. J. Shields, M. Cardona, R. Nötzel, and K. Ploog, Phys. Rev. B **46**, 10 490 (1992).
[16]J. Hegarty, M. D. Sturge, C. Weisbuch, A. C. Gossard, and W. Wiegmann, Phys. Rev. Lett. **49**, 930 (1982).
[17]Superlatt. Microstruct. **6**, 271 (1989).